The effect of pH and dissolved inorganic carbon on the properties of iron colloidal suspensions

Darren A. Lytle and Vernon L. Snoeyink

ABSTRACT

Discoloured water resulting from suspended iron particles is a relatively common drinking water consumer complaint. These particles result from the oxygenation of Fe(II), and this study shows that pH and dissolved inorganic carbon (DIC) have important effects on their properties. Bench scale tests were conducted at a single oxygen concentration over a broad pH range. Increasing the DIC concentration increased the turbidity and apparent colour of a fixed concentration of iron suspension below pH~8.7. Inorganic carbon was incorporated into the particle structure at these pH values. Above pH~8.7 and in higher DIC waters, an intermediate green solid that contained Fe(II), Fe(III) and inorganic carbon formed for a brief period prior to complete oxidation to an Fe(III) solid. The green solid apparently was green rust, $Fe^{II}_4Fe^{III}_2(OH)_{12}CO_3$. After complete oxidation of the intermediate solid to an Fe(III) solid, the iron particles did not include measurable amounts of inorganic carbon and appeared to maintain the physical structure of the green rust. Above pH~8.7, DIC did not affect suspension colour and turbidity and inorganic carbon was not incorporated in the particle structure. The colour and turbidity of iron suspensions were largely related to particle size distribution.

Key words | colloids, colour, drinking water, inorganic carbon, iron, turbidity

Darren A. Lytle (corresponding author)
US Environmental Protection Agency,
NRMRL, WSWRD, TTEB,
26 W. Martin Luther King Dr.,
Cincinnati,
Ohio 45268,
USA
Tel: 513 569 7432
E-mail: *lytle.darren@epa.gov*

Vernon L. Snoeyink
University of Illinois,
Urbana-Champaign,
Illinois,
USA

INTRODUCTION

'Red water' is a relatively common consumer complaint received by many drinking water utilities. Red water describes the appearance of drinking water that contains suspended particulate iron, although the actual suspension colour may be light yellow to brown depending on water chemistry and particle properties. The U.S. Environmental Protection Agency has issued a secondary maximum contaminant level (SMCL) for iron of 0.3 mg/l based on aesthetic issues (Pontius 1992). Iron in water does not pose a known human health risk, but adsorbed trace impurities such as metals, organic compounds and microorganisms may cause adverse health effects.

Iron can originate from the source water and from distribution system materials. The relatively soluble +II oxidation state is the dominant form of iron in anoxic environments including some groundwaters, the hypolimnion of stratified eutrophic reservoirs, drinking water in iron distribution system dead ends, and the region beneath thick iron corrosion scales. Upon exposure to oxygen or disinfectant during water treatment and distribution, Fe(II) is oxidized to insoluble Fe(III), which readily precipitates and is responsible for coloured water.

The structure and properties of iron oxyhydroxide (hydrous iron oxide) colloids in aquatic systems have been studied extensively because of their abundance in environmental and engineered systems, and their important sorption properties such as their large surface area and surface chemistry. The adsorption of trace inorganic constituents (Pierce & Moore 1980; Waychunas, G. A. *et al.* 1993*a, b*; Edwards 1994; Waychunas *et al.* 1995; Kovacevic *et al.* 2000), nutrients such as phosphate (Gshwend & Reynolds 1986; Odum 1988; Machesky *et al.* 1989; Buffle *et al.* 1989; Chambers & Odum 1990; Seamon *et al.* 1997) and organic compounds (Tipping & Cooke 1981; Davis 1982; Zinder

et al. 1986; Yost *et al.* 1990; Tejedor-Tejedor *et al.* 1992; Gu *et al.* 1994) onto iron oxyhydroxides have been studied. The adsorptive characteristics are important in wastewater and drinking water treatment systems that use or remove iron, and in the transport of contaminants through groundwaters and surface waters.

Synthetic iron oxyhydroxides are often generated under controlled laboratory conditions to simulate natural material. As a result, a number of investigators have compared the nature of synthetic and natural oxyhydroxides (Landa & Gast 1973; Schwertmann & Fischer 1973; Carlson & Schwertmann 1981; Crosby *et al.* 1983). Factors such as age, iron concentration and water chemistry can affect the properties of iron particles, and can contribute to variability between field and experimental observations. The process pathway in which the solids form must also be considered. Adsorption studies have been conducted using Fe(III) solids or solids derived from the hydrolysis and precipitation of Fe(III) salts. Although this approach to forming iron particles provides important information, the formation of Fe(III) oxyhydroxides in many environmental systems is often initiated from the oxidation of Fe(II). The physical and chemical characteristics of Fe (III) precipitates originating from Fe(II) differ from those originating from dissolved Fe(III) (Crosby *et al.* 1983). The time of introduction of materials that react with the iron solid is also important. In many laboratory studies, cations, anions or organic materials are added after Fe(III) precipitation. In natural systems, these materials are typically present during Fe(II) oxidation and particle nucleation. The latter setting has been demonstrated to yield particles with higher sorption capacities (Laxen 1985; Fuller *et al.* 1993). The presence of dissolved species that react with the solid as it is being formed can impact the surface properties of the iron solids by inhibiting crystal or floc growth (Mayer & Jarrell 2000) and by affecting surface charge, which in turn impacts adsorption properties (Schwertmann & Thalmann 1976; Schwertmann & Cornell 1991).

Although the properties of iron colloids have been studied in aqueous environments, none of these studies have been conducted using the water chemistry, iron concentration, and other conditions experienced in drinking water treatment and distribution systems. In addition, the effect of water chemistry on the aesthetic properties of iron suspensions has not been studied and particle properties have not been related to suspension properties such as turbidity and colour. The objective of this research was to evaluate the effect of pH and DIC on the properties of iron particles and the aesthetic properties of the corresponding suspensions derived from the oxygenation of Fe(II).

MATERIALS AND METHODS

Reaction cell

Iron particles were formed in a 1.2 litre glass reaction vessel. The top of the cell contained ports for a pH electrode, a dissolved oxygen/temperature probe, a mechanical stirrer, a gas feed tube, injection of acid and base, and sampling. A computer software-controlled dual titrator system (Schott Geräte, Germany) was used to maintain a constant pH by rapidly adding small increments of acid or base to compensate for pH changes brought about by the addition of Fe(II) and chemical reactions. The computer software (Jenson Systems, Hamburg, Germany) recorded pH values and titrant volumes that were maintained in a data file.

Water and chemicals

Double deionized (DDI) water was prepared by passing distilled water through a Milli-Q Plus© cartridge deionized water system (Millipore Corp., Bedford, MA), having a resistivity ≥18.2 MΩ · cm.

Unless otherwise specified, all chemicals used in this study were Analytical Reagent (AR) grade. The amount of ultrapure nitric acid, HNO_3 (Ultrex, J. T. Baker Chemical Company, Phillipsburg, NJ) used to preserve samples for metals analysis was 1.5 ml/litre sample. Dilute 0.6 M HCl (Mallinckrodt, Inc., Paris, KY) and 0.5 N NaOH (Fisher Scientific, Fairlawn, NJ) were used to adjust the pH. Sodium bicarbonate (Fisher Scientific, Fairlawn, NJ) was added to the cell to adjust water quality. Iron was

added as ferrous sulphate ($FeSO_4 \cdot nH_2O$)[1] (Fisher Scientific, Fairlawn, NJ).

Analytical methods

The pH was measured with a Hach Company (Loveland, CO) EC40 benchtop pH/ISE meter (model 50125) and a Hach Company (Loveland, CO) combination pH electrode (model 48600) with temperature corrections. The instrument was standardized daily using a two-point calibration with pH 7 and 10 standard solutions (Whatman, Hillsboro, OR). Dissolved oxygen (DO) was measured with a Hach Company (Loveland, CO) Model DO175 dissolved oxygen meter and a Model 50180 dissolved oxygen probe. Total iron was analysed with a Thermo Jarrel Ash (Franklin, MA) 61E® purged inductively coupled argon plasma spectrometer (ICAPS). Colour, ferrous iron and total iron were measured with a Hach DR/2000 spectrophotometer (Loveland, CO). Ferrous iron was measured using the 1,10 phenanthroline method (Hach Company 1990; APHA-AWWA-WEF 1995). Total iron was measured by the same method except that a reducing reagent was also included in the reagent powder pillow provided by the Hach Company to convert Fe(III) to Fe(II). Turbidity was measured using a Hach 2100N turbidimeter. Dissolved inorganic carbon (DIC) was analysed by a coulometric procedure on a UIC Model 5011 CO_2 coulometer (Joliet, IL) with Model 50 acidification module, operated under computer control. Syringe filters (0.45, 0.2, 0.02 μm) (Whatman, Inc., Clifton, NJ) were used to separate colloidal iron during colour and iron measurements.

Other

Glassware (excluding pipettes) used for the preparation of standards and solutions was cleaned using a 5% solution of Contrad 70©. The glassware was thoroughly rinsed with deionized water. Reused glassware was immediately cleaned by soaking in 10% (v/v) concentrated HNO_3 and rinsed with DDI H_2O. Air displacement micropipettes with disposable tips were used for handling and transferring solutions.

Experimental procedure

Experiments were initiated by adding 1 litre DDI water to the reaction cell. A 12.2%:87.8% O_2:N_2 gas mixture (Praxair, North Royalton, Ohio) was bubbled through the water until the dissolved oxygen concentration stabilized ($PO_2 = 0.122$ atm, dissolved oxygen ~5 mg/l). The gas tube was then positioned just above the water surface. The water was mixed using a mechanical stirrer and plexiglass paddle (one 19 mm radius blade) at 20 rpm ($G = 3.5\ sec^{-1}$). An appropriate amount of sodium bicarbonate was then added to the water. The titration system was programmed to the desired pH and started. After the pH stabilized, ferrous sulphate was added to give an initial ferrous iron concentration of approximately 1 mg/l (1.79×10^{-5} M) or 5 mg/l (8.95×10^{-5} M) depending on the goal of the test run. The tendency for pH to change during test runs due to oxidation and precipitation reactions, and CO_2 transfer was countered by the titration system. Inorganic carbon changes due to CO_2 transfer between the test water and atmosphere were measured during typical experiments at pH 7, 8, 9 and 10 in waters containing 5 and 100 mg C/l DIC. Significant changes were noted only at pH 7 (both DIC conditions) where 5% DIC decreases were observed. Samples were drawn out of the cell with a syringe approximately 20 min after complete oxidation of Fe^{2+} had taken place. A separate parallel study was dedicated to determining the effect of water chemistry on the oxygenation kinetics of Fe(II). Oxygenation rate experiments were performed using the same apparatus, conditions and water chemistries used in the particle generation experiments. During each test run, 15 ml samples were periodically drawn from the reaction cell using a 20 ml syringe that was prefilled with 5 ml of 0.6% HNO_3 (necessary to quench oxidation reaction). The samples were analysed for ferrous iron and the results were later used to develop oxygenation rate relationships. Mixing duration beyond approximately 5 min after

[1]The purchased material was listed as $FeSO_4 \cdot 7H_2O$ (Fisher Scientific), however, X-ray diffraction analysis and titrometric standardization of stock solution indicated that the original chemical dehydrated over time. Analysis showed that $FeSO_4 \cdot 7H_2O$, $FeSO_4 \cdot 4H_2O$ and $FeSO_4 \cdot H_2O$ were present and that the chemical dehydration accounted for about a 10% error in the final stock solution concentration.

complete Fe(II) oxidation did not significantly impact the colour and turbidity of iron suspensions.

Transmission electron microscope

Transmission electron micrographs (TEM) were obtained using a Jeol 1200 EX electron microscope (Japan) operated at 80 kV at various degrees of magnification. Elemental analysis was done using a Oxford Link EXL energy dispersive X-ray spectrometer (EDS) (Oxford, UK).

TEM sample preparation procedure

Conventional centrifugation was used to concentrate colloidal iron particles (Perret *et al.* 1991). Glass pipettes were used to withdraw 10 ml iron colloid suspension samples from the glass reactor vessel. The sample was immediately transferred to a 15 ml centrifuge tube, and centrifuged in a microcentrifuge for 5 min at 5000 rpm to concentrate the colloids. Following centrifugation, the sample was mixed with NANOPLAST® FB101 which is a hydrophilic melamine resin (Bachhuber & Frosch 1983). Nanoplast resin embedding of aquatic colloids has been shown to provide minimally perturbed images of aquatic colloidal structures (Frosch & Westphal 1989; Perret *et al.* 1991; He *et al.* 1996). The melamine resin was prepared and mixed with the concentrated sample according to the supplier's instructions. Typically, 0.1 ml of resin was mixed with 1 ml of sample taken from the bottom of the centrifuge tube.

Mixed samples were directly deposited on carbon coated copper TEM grids based upon the technique suggested by Nomizu & Mizuike (1986). The grid was heated at 40°C for 48 h followed by 48 h at 60°C, and finally at 70°C for 12 to 24 h (He *et al.* 1996).

X-Ray diffraction

X-Ray diffraction (XRD) was used to identify crystalline phases. Colloids and particles were filtered from suspension onto a 47 mm diameter 0.45 μm filter (Millipore Corp., Bedford, MA) or a 0.1 μm filter (Costar Corp., Cambridge, MA) using a vacuum filtration apparatus. The filter was immediately placed in the instrument and the solid material was analysed before drying. A Scintag (Scintag, Inc., Santa Clara, CA) XDS-2000 theta-theta diffractometer with a copper X-ray tube was used to acquire X-ray patterns. Pattern analysis was performed using the computer software provided by the manufacturer which generally followed ASTM procedures (ASTM 1996).

Electrophoretic mobility

The electrophoretic mobility (EPM) of iron colloids was measured using a Malvern Zetasizer 4 (Malvern Instruments Ltd, Malvern, U.K.). The instrument measures the EPM by laser doppler electrophoresis and is expressed as a velocity divided by the applied field to give EPM expressed in units of μm cm V^{-1} s^{-1}. The EPM is used by the computer software to calculate the zeta potential using the Smoluchowski relationship (Hunter 1981). James (1991) described the relationship between electrophoretic mobility and zeta potential, and noted complications that arise from making assumptions about the variables used in the calculation of zeta potential. For example the high concentration of ions near the charged surface, and the viscosity and relative permittivity in the electrical double layer may differ from that of the bulk solution. Since variables used to derive the zeta potential are based on the bulk solution characteristics, uncertainties on the zeta potential may exist. Particle size and shape assumptions must also be made in the conversion. Therefore, electrokinetic properties are reported in this manuscript as the measurable parameter of electrophoretic mobility to eliminate these uncertainties. Negative electrophoretic mobility values represent particle movement in the direction of the anode and a net negative surface charge.

Samples were injected directly into the 1.5 ml quartz capillary measurement tube with 10 ml disposable syringes. New syringes were used for each sample. Prior to the measurement of each new sample, approximately 20 ml of deionized water was rinsed through the cell followed by a 10 ml rinse with the sample to be measured.

Subsequent replicate measurements (typically four to five depending on sample volume) were made after 4 ml injection increments. The instrument was checked daily using a MIN-U-SIL© (ground crystalline silica powder) suspension prepared by adding 0.02 g of MIN-U-SIL© to 200 ml filtered distilled water (Bier 1959). Measurements were made within 30 min of particle formation and at 25°C.

Particle counting and sizing

Particles (<1 μm diameter) were sized with a Malvern Zetasizer 4 (Malvern Instruments Ltd, Malvern, U.K.). The instrument sizes (average diameter) particles using photon correlation spectroscopy (PCS) which measures Brownian motion and relates it to the size of particles. A He-Ne laser (wavelength 633 nm) is passed through the sample. Scattered light is detected by a photomultiplier. Fluctuations in the intensity of scattered light due to moving particles in the beam are converted to electrical signals. The signals pass a correlator and are sent to a computer where the information is analysed and converted to size information using light scattering theory. Particle counts and sizing (>1 μm diameter) were measured with a Pacific/Scientific HIAC/ROYCO (Silver Springs, MD) model ABS particle counter. The instrument uses laser light obscuration technology to size and count particles.

RESULTS AND DISCUSSION

Iron particles were formed using solutions with dissolved inorganic carbon (DIC), dissolved oxygen, pH and iron concentration that represent the chemistry of water in drinking water distribution systems. Ferric iron particles were generated by reacting oxygen with ferrous iron. The intent was to create a condition similar to that in distribution systems when Fe(II) is released from the pipe wall to anoxic water, followed by oxidation when it comes into contact with oxygen. The particle formation approach used in this study is also representative of iron-containing anoxic waters after the introduction of oxygen. Also, it should be noted that the terms 'particle' and 'colloid' are used interchangeably in this paper although technically colloid may be defined as a subset of particles having a diameter less than 1 μm.

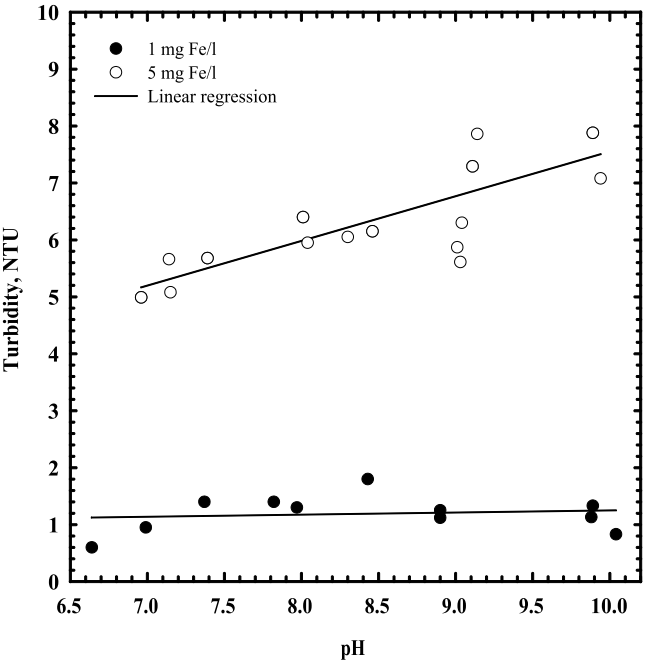

Figure 1 | The effect of pH and iron concentration on suspension turbidity (5 mg C/l, PO_2=0.122 atm, 23°C).

Suspension turbidity and colour

Iron (III) particles were formed in solutions containing 5, 50 and 100 mg C/l of DIC (4.17×10^{-4} M, 4.17×10^{-3} M and 8.34×10^{-3} M sodium bicarbonate), and iron concentrations of 1 and 5 mg/l, over a pH range of 6 to 10. The effect of pH on turbidity formation in water with 5 mg C/l is shown in Figure 1. The 1 mg/l iron suspension turbidity was scattered between 0.5 to 1.5 NTU over a pH range of 6.6 to 10. The turbidity of 5 mg/l iron solutions increased from approximately 5 to 8 NTU as pH increased from 7.0 to 10. The five-fold increase in iron concentration resulted in roughly a five-fold increase in turbidity. Figure 2 shows that turbidity increased linearly with increasing iron concentration up to 30 mg/l at pH 7.5. The rate of

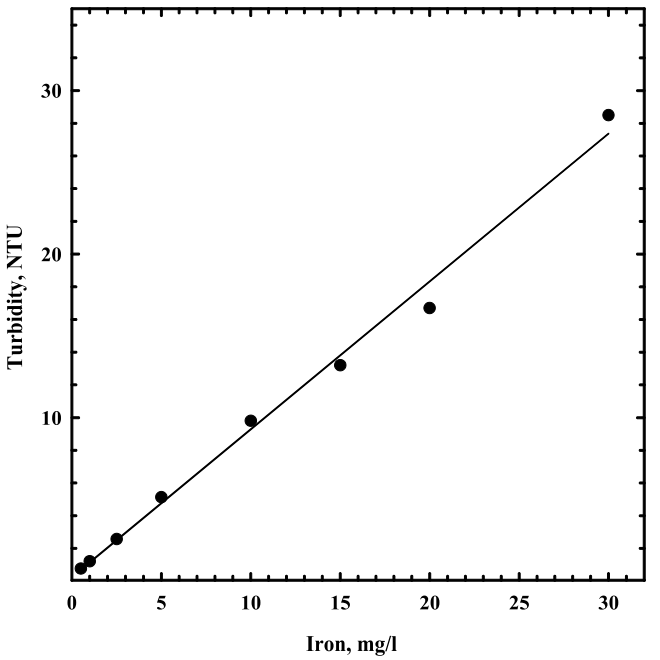

Figure 2 | The effect of iron concentration on the turbidity of iron suspensions (pH=7.5, 5 mg C/l, 22°C, PO_2=0.122 atm).

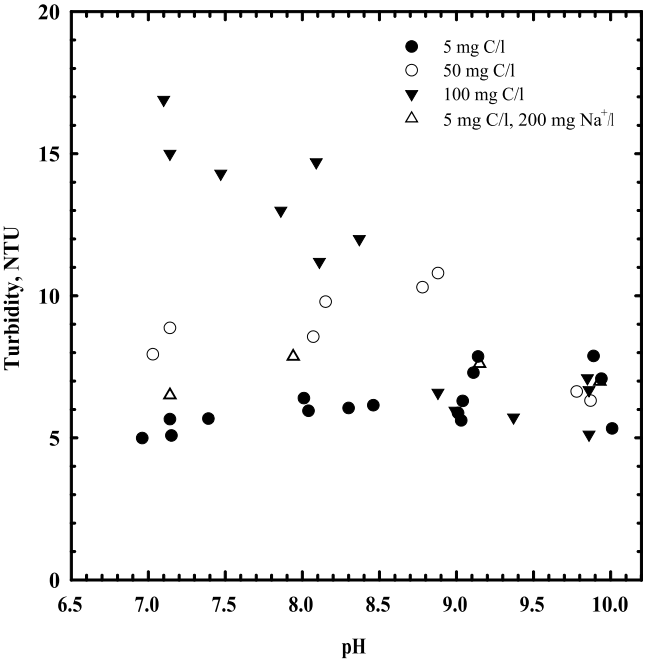

Figure 3 | The effect of pH and DIC on the turbidity of 5 mg/l iron suspensions (PO_2=0.122 atm, 23°C).

increase of turbidity was 0.9 NTU per mg Fe/l (R^2 = 0.993).

Increasing the DIC from 5 to 50 mg C/l increased the turbidity of 5 mg Fe/l suspensions by 3 to 4 NTUs when the pH was equal to and below 9, but had essentially no effect on the turbidity at pH 9.8 and 9.9 (Figure 3). Further increasing the DIC to 100 mg C/l increased the turbidity by an additional 4 to 5 NTUs when the pH was below 8.5, but again had no effect on the turbidity compared to the 5 mg C/l suspension above about pH 8.5.

A set of experiments was conducted to determine whether ionic strength differences amongst the DIC-containing waters explained the observed turbidity differences. Ionic strength differences due to additional sodium from sodium bicarbonate and sodium hydroxide (pH adjustment), and chloride (pH adjustment) between the 5 mg C/l and 100 mg C/l suspensions were approximated. The 5 mg DIC/l experiments were repeated with the addition of sodium chloride (prior to iron addition) to a concentration of 200 mg Na/l and an ionic strength similar to the 100 mg C/l suspensions. There appeared to be a small increase in turbidity (less than 1 NTU) at pH of 7 and 8 due to the addition of sodium chloride (Figure 3), but this amount was far less than the turbidity differences between the 5 mg C/l and 100 mg C/l DIC iron suspensions.

The presence of large pale-green coloured particles in the reaction cell was typically observed immediately after the addition of ferrous sulphate when pH was above 8.5 and the DIC was 50 and 100 mg C/l. The green solids changed to yellow in as little as 15 to 30 sec, suggesting that an unstable intermediate iron solid phase existed for a brief period. The physical characteristics of the particles formed above and below pH 8.5 were examined by transmission electron microscopy (Figure 4). Particles formed at low pH had webbed features and some suggestion of edges indicating poorly ordered crystalline features (Figure 4a). Particles formed from the intermediate green particles appeared as granular clusters (Figure 4b). Examination under high magnification revealed individual grains with sharp edges and dimensions in the order of 150 to 200 nm.

The effect of iron concentration and pH on apparent colour of 5 mg C/l suspensions is shown in Figure 5. The apparent colour (unfiltered samples) of 1 mg/l iron

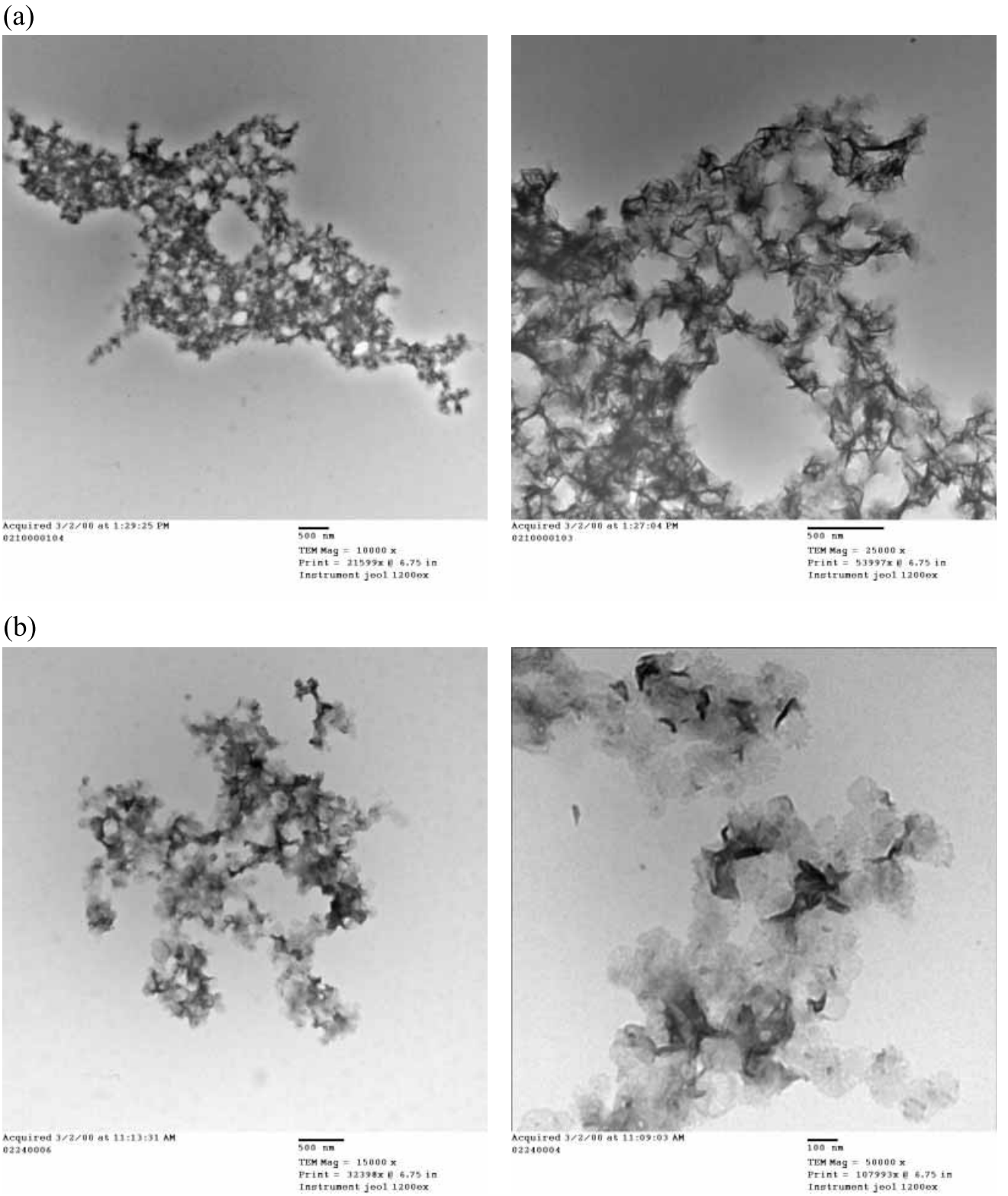

Figure 4 | Transmission electron micrographs of iron particles (5 mg Fe/l, 23°C, PO_2=0.122 atm, 100 mg C/l DIC) at pH (a) 7.5 (no green solid observed) and (b) 9.35 (green solid observed).

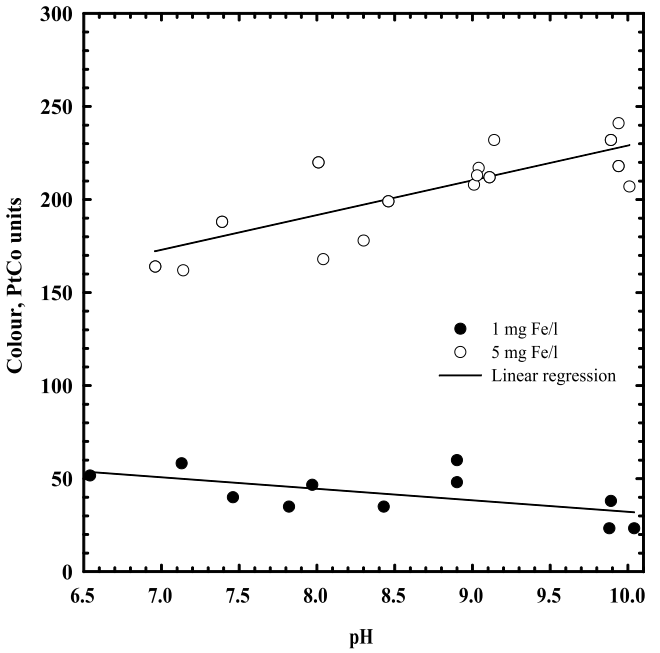

Figure 5 | The effect of pH and iron on the apparent colour of iron suspensions (5 mg/l DIC, PO_2=0.122 atm, 23°C).

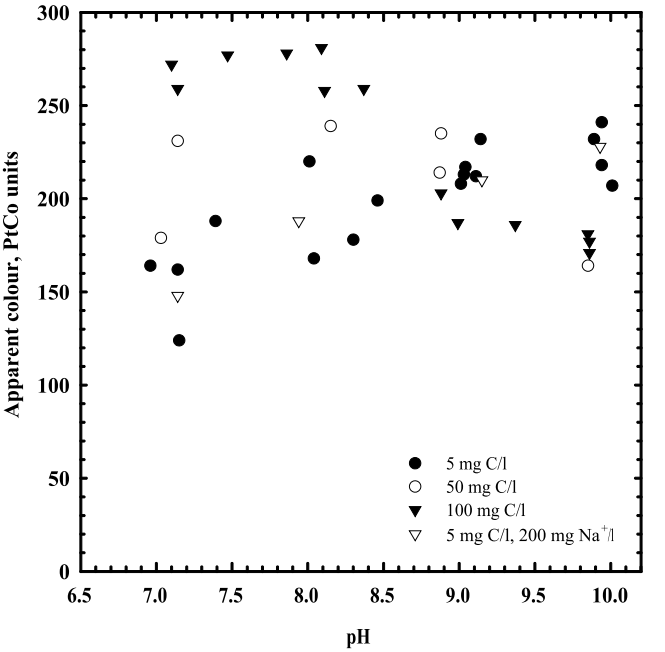

Figure 6 | The effect of DIC on the apparent colour of 5 mg/l iron suspensions (PO_2=0.122 atm, 23°C).

suspensions slightly decreased with increasing pH based on linear regression analysis and ranged from approximately 30 to 65 PtCo units between pH 7 and 10. The apparent colour of the 5 mg/l iron suspensions gradually increased from approximately 165 to 230 PtCo units as pH increased from 7 to 10, similar to the way that turbidity increased as pH increased. The effect of iron concentration on colour paralleled turbidity. Increasing the iron concentration by a factor of 5 caused an increase in apparent colour by a factor of 4 to 5. Additional experiments using other iron concentrations conducted at pH 7.5 and 5 mg C/l showed that apparent colour increased linearly with increasing iron concentration up to 30 mg Fe/l at a slope of 37 PtCo units per mg Fe/l ($R^2 = 0.998$, graph not shown).

Increasing the DIC concentration from 5 to 50 mg C/l by adding sodium bicarbonate appeared to slightly increase apparent colour below pH 9 (Figure 6). Increasing the DIC concentration to 100 mg C/l caused a suspension colour increase of approximately 75 PtCo units below pH 8.5 over the 5 mg C/l DIC suspensions (Figure 6). At pH values of 8.5 and higher, apparent colour decreased rapidly to about 50 PtCo units below the value for the 5 mg C/l DIC suspension at pH 10. The addition of 200 mg Na/l to the 5 mg C/l test water did not affect the apparent colour of iron suspensions.

True colour (0.45 μm filtered samples) of 1 mg/l iron suspensions (5 mg C/l) was typically less than 50% of the apparent colour and averaged approximately 25 PtCo units over the evaluated pH range (data not shown). The exception was at pH 10 where nearly 100% of the colour passed the filter. Measurable colour was not detected following filtration of these suspensions through 0.2 μm filters. The colour of 5 mg/l iron suspensions (5 mg C/l) did not pass through a 0.45 μm filter below pH 8 (Figure 7) as did the particles from the 1 mg Fe/l suspension. This difference reflects a larger particle size possibly caused by increased particle collision frequency as a result of the larger iron solid concentration. However, true colour (0.45 μm) increased rapidly above pH 8. At pH 10, approximately 65% of the colour passed through a 0.45 μm filter. No detectable colour passed through a 0.2 μm filter at any pH. True colour (0.45 μm filtered suspensions) of 50 mg C/l suspensions increased from pH

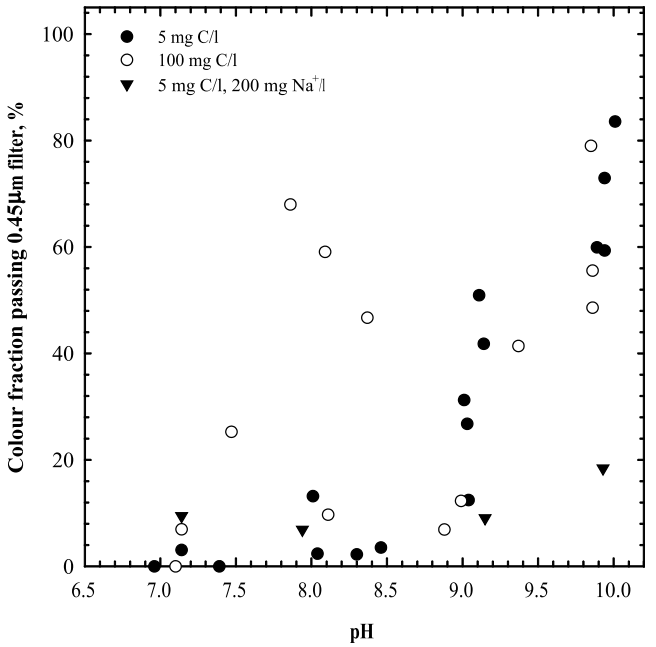

Figure 7 | The effect of pH and DIC on the filterable colour of 5 mg/l iron suspensions (23°C, PO_2=0.122 atm).

7 to 8, decreased from pH 8 to 9, and increased from pH 9 to 10 (data not shown). No colour passed the 0.2 μm filter. True colour (0.45 μm filtered suspensions) of 100 mg C/l suspensions was observed at all pH values (Figure 7). Like the 50 mg C/l true colour trend, there were colour peaks at pH 8 and 10 (assuming data point at pH 8.1 was an outlier), and no colour passed a 0.2 μm filter. DIC did not significantly impact the fraction of colour passing a 0.45 μm filter above pH 9. The filtered colour data imply that increasing the DIC decreased the size of iron particles below pH 8 to 8.5. The size differences between iron particles formed in different DIC-containing waters corresponded well with the observed differences in turbidity and colour, which suggests that particle size contributed to the differences.

The addition of 200 mg Na/l to the 5 mg C/l test water did not affect the apparent colour of iron suspensions (Figure 7) but did have an effect on the 0.45 μm filtered colour at pH 9 and 10. The presence of sodium chloride at pH 10 decreased the amount of colour passing the filter from approximately 75% to 25%. The observations suggest that sodium cations had a coagulating effect on the iron particles.

Particle composition

A series of experiments was conducted to determine whether inorganic carbon was incorporated in the structure of the iron particles, and to identify the short-lived green solid formed in higher pH and DIC waters. The incorporation of inorganic carbon in the iron particles was determined by comparing total inorganic carbon, DIC concentrations (dissolved plus particle-associated inorganic carbon), of suspensions prior to and after filtration through 0.2 μm filters. The method and instrument used to make inorganic carbon measurements produced highly precise and accurate data that permitted distinction between small differences. The precision of the DIC analysis was determined by pooling historical data collected since 1998. The pooled standard deviation (SD) about the mean (Skoog & West 1963) of 138 sets of duplicate real DIC samples in the concentration range of 4 to 9 mg C/l collected between February 2001 and January 2002 was 0.06 mg C/l. The SD of 184 pairs of samples in the concentration range of 9 to 23 mg C/l collected between April 2000 and January 2002 was 0.10 mg C/l. The SD about the mean of 79 duplicate sets of DIC samples in the concentration range of 37 to 100 mg C/l collected between March 1998 and December of 1999 was 0.51 mg C/l. Loss of inorganic carbon due to degassing during filtration was also considered in an independent study prior to the particle composition study. Waters containing 5 and 100 mg C/l DIC at several pHs (no iron) were filtered as usual. No measurable differences in post- and pre-filtered DIC water sample measurements were noted.

Particle suspensions containing 5 mg Fe/l and 50 mg C/l DIC at pH 7.1 and 8.9 after all Fe (II) had been oxidized were analysed. The particles contained 0.25 mg C/l at pH 7.1 which is equivalent to an Fe:C molar ratio of 4.3:1. No measurable inorganic carbon was detected in iron particles at pH 8.9. The experiment was repeated at pH 7.14 using 20 mg Fe/l. The particles contained 0.96 mg C/l and had an Fe:C molar ratio of 4.7:1. Five mg/l iron suspensions were formed in 100 mg C/l DIC solutions at

pH 7. The amount of inorganic carbon associated with the iron particles increased to 1.06 mg C/l which was equivalent to a Fe:C molar ratio of 1.

An experiment was conducted at pH 9.92 using 20 mg Fe/l and 50 mg C/l to determine the composition of the short-lived green particles and the final oxidation product. Samples were drawn from the reaction cell at approximately 15 and 30 sec after ferrous iron was added, during the period when the green material was observed, and after 35 min when yellow particles were observed. Ferrous iron, total iron and inorganic carbon were measured. Ferrous iron samples were taken by drawing 15 ml samples from the test cell using a 20 ml syringe prefilled with 5 ml of 0.6% HNO_3 (Mallinckrodt, Inc., Paris, KY) at appropriate time intervals. Acid was necessary to bring the pH to 3 to 4 and quench the oxidation reaction. The sample was analysed for ferrous iron within 10 min of sampling. All iron was in the particulate form at the time of sampling. Ferrous iron concentration in the particles decreased from 11.8 to 8.5 mg/l as the time of reaction increased from 15 to 30 sec. During the same time frame, inorganic carbon in the solid phase dropped from 1.6 mg C/l to 1.1 mg C/l. Siderite, $FeCO_3$, was oversaturated at the time of Fe(II) addition based on chemical modeling (van Gaans 1989), however, the saturation state of iron changed rapidly as oxidation took place. Although siderite may have theoretically been the stable Fe(II) solid phase, the observed green-coloured solid was not in agreement with the reported colour of siderite. A more reasonable guess of the identity of the solid was green rust ($Fe_4^{II}Fe_2^{III}(OH)_{12}CO_3$). Assuming that all ferrous iron and inorganic carbon were incorporated in a green rust-like solid (Fe(II):Fe(III) of 2:1) and that OH- was necessary to create a neutral solid, a hypothetical solid having the formula $Fe_4^{II}Fe_2^{III}(OH)_{8.87}(CO_3)_{2.56}$ was present after 15 sec. In order to account for all of the ferric iron, a solid containing 2.51 mg Fe(III)/l was also present. After 30 sec, the calculated solid formula remained nearly the same, $Fe_4^{II}Fe_2^{III}(OH)_{9.12}(CO_3)_{2.44}$, but the amount of ferric solid had increased to 10.5 mg Fe(III)/l. The suspension was analysed again after all of the iron was oxidized to Fe(III) (35 min). The particles no longer contained measurable amounts of inorganic carbon, showing that the green solid had been completely oxidized.

Additional experiments were conducted in an "oxygen-free" glovebox to slow the transformation of Fe(II)-Fe(III) solid to a ferric solid and positively identify the green solid. Test waters were prepared as described above. Oxygen was removed by nitrogen stripping until the dissolved oxygen concentration was minimized. The reactor cell was then transferred to the glovebox and remaining oxygen was stripped from the test water using a gas recirculation pump. Ferrous iron was added after the dissolved oxygen reading was reduced typically to a reading of zero. It was not possible to put the pH controller into the glovebox because of its size and thus pH could not be kept constant as in the other experiments. However, pH, dissolved oxygen, ferrous iron and total iron (filtered and non-filtered) were monitored. A green solid formed in high pH waters shortly after the addition of ferrous iron in 5, 50 and 100 mg C/l solutions. Iron analysis showed that some Fe(II) had been oxidized to Fe(III) even though no oxygen was detectable indicating that the atmosphere was not truly oxygen-free. The Fe(II):Fe(III) ratio dropped in an exponential manner from 10 to 0.2 over a period of 9 days. The green solid formed in the glovebox visually appeared to be the same material that formed during the bench experiments. The green solid was formed in 5 mg C/l DIC water in the glovebox even though it was not observed at this DIC concentration in experiments conducted at $PO_2 = 0.122$ atm. The solid was filtered and quickly analysed by X-ray diffraction (XRD). The solid remained green for several minutes outside the glovebox before gradually turning yellow. XRD analysis of the solid formed in 5 mg C/l DIC solution after being in the glovebox for 26 days showed that the only identifiable crystalline phase was green rust, $Fe_4^{II}Fe_2^{III}(OH)_{12}CO_3$ (see Figure 8a) (Hansen 1989). The same solid was identified in the 100 mg C/l DIC (pH 9.65 to 9.86) solution after nearly 6 days (Figure 8b). Finally, an analysis of the 50 mg C/l DIC (pH 9.65) suspension that had been in the glovebox for 57 days showed the presence of green rust and lepidocrocite (Figure 8c), which are reported oxidation products of Fe(II) (Schwertmann & Fechter 1994; Drissi *et al.* 1995; Legrand *et al.* 2000). Poorly crystalline magnetite may also have been present based on the observation that the suspension appeared black and black particles were attached to a magnetic stirrer bar. The results showed that

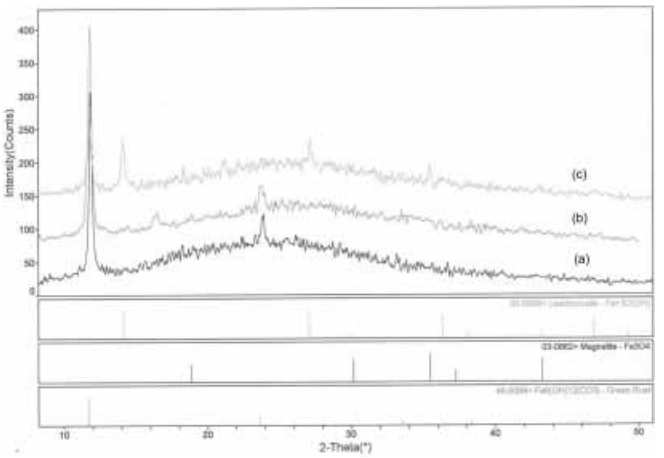

Figure 8 | X-ray diffraction analysis of ''green rust'' collected during glovebox experiments at (a) pH 9.5 and 5 mg C/l DIC after 26 days, (b) pH 9.65 to 9.86 and 100 mg C/l DIC after 6 days, and (c) pH 9.65 and 50 mg C/l DIC after 57 days.

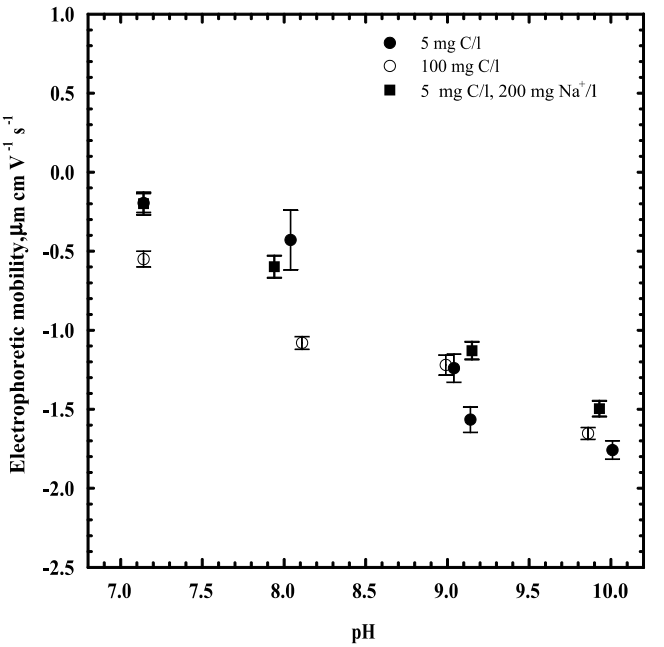

Figure 9 | The effect of pH, inorganic carbon and sodium on the electrophoretic mobility of suspended iron particles (5 mg Fe/l, PO_2=0.122 atm, 22°C).

the formation of green rust is highly sensitive to pH, DIC and oxygen concentration. Although siderite was predicted to be the most stable iron phase (van Gaans 1989) in the glovebox conditions, no sign of the mineral was ever detected. Drissi *et al.* (1995) reported similar observations in their work on green rust and suggested that the formation of siderite may be limited by kinetic constraints.

Electrophoretic mobility

Figure 9 shows the electrophoretic mobility (EPM) of freshly formed iron (III) particles as a function of pH in 5 and 100 mg/l DIC waters. The EPM of particles in the 5 mg C/l water became more negative with increasing pH to a maximum negative value of -1.5 μm cm V^{-1} s^{-1} at pH 10. Increasing EPM toward the positive electrode means that the net surface charge of the iron particles increased in the negative direction with increasing pH. This trend can be explained by the increased tendency for the dissociation of surface groups with increasing pH. The increase in negative EPM corresponded with the observed increase in filterable colour (and particle size), which suggests that electrostatic force interactions affected particle aggregation and growth. The point where the EPM was zero or the point of zero charge (PZC) was not reached in the experimental pH range, but was projected to be between pH 6.5 and 7. A range of PZC values of 4.2 to 7.2 for goethite (α-FeOOH) and 5.3 to 7.4 for lepidocrocite (γ-FeOOH) has been reported (Parks 1965). Variability in reported values may be due to many factors including experimental conditions, electrolyte concentration, adsorbed impurities, structural imperfections and state of hydration. Increasing the DIC from 5 to 100 mg C/l did not have a significant effect on the EPM of iron particles at pH 9 and 10, and appeared to slightly decrease the EPM at pH 7 and 8. The presence of 200 mg Na/l in the 5 mg C/l solutions also did not affect the EPM of iron particles.

Colloid/particle size and counts

Size measurements of iron particles suspended in sodium bicarbonate buffered waters were unsuccessful. Suspensions were relatively unstable and tended rapidly to form visible flocs, particularly below pH 9. Particle size measurements were uncertain because the particles

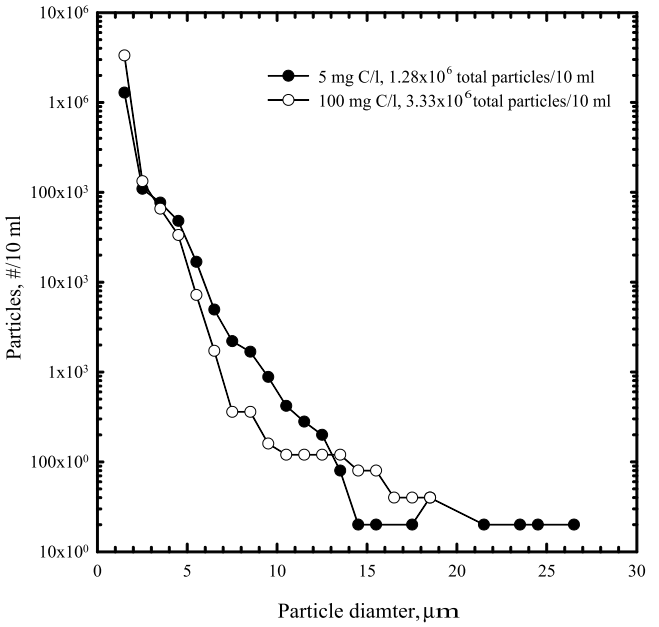

Figure 10 | The effect of DIC (mg C/l) on particle counts (>1 μm) and particle size distributions of iron suspensions at pH 7.5 (PO_2=0.122 atm, 23°C).

tended to settle in the instrument sample chamber during the size measurement.

Particle sizing and counting of particles greater than 1 μm in diameter showed that there were differences between the distribution and numbers of particles formed in waters containing 5 and 100 mg C/l DIC at pH 7.5 (Figure 10). The 100 mg C/l suspensions contained approximately 2.3 times as many total particles as the 5 mg C/l suspension. The major difference in particle counts was in the 1 to 3 μm diameter size range where the 100 mg C/l suspension contained many more particles. The 5 mg C/l suspension contained a greater number of particles in larger size ranges. These data suggested that particles formed in 100 mg C/l suspension had a smaller average diameter. This conclusion was also supported by the colour data discussed earlier (Figure 7) and the filtered iron data.

Suspension stability

The stability of iron suspensions was determined by visual examination. Stabile suspensions were defined as those that did not precipitate or form visible solids and remained discoloured for longer than 24 h. The impact of pH on the stability of aqueous solutions containing 5 mg/l iron and 5 mg C/l DIC was evaluated by examining undisturbed glass vials of the suspensions. Increasing the pH increased the stability of the suspension. Suspensions formed at approximately pH 7 and 8 were unstable, with the solids forming an orange-coloured floc at the bottom of the vial. A mixture of stable particles and settled floc was present at pH 9. Dark orange floc was observed at the bottom of the vial and the water above was light yellow in colour. The pH 10 suspension was stable. The increase in suspension stability with increasing pH was attributed to the corresponding negative EPM increase (Figure 9) which is predicted to decrease particle-particle interactions. Increasing the DIC to 50 and 100 mg C/l did not produce stabile suspensions at pH 7 and 8, and in most instances reduced the stability of suspensions at higher pH values. Large floc was typically observed in the reaction cell during the particle formation experiments at all pH values when the DIC was 50 and 100 mg C/l. The loss of stability was thought to be attributed to the coagulating effect of the additional sodium ions associated with $NaHCO_3$ used to increase DIC. Increasing the DIC from 5 to 50 and 100 mg C/l resulted in sodium increases of nearly 90 and 180 mg/l, respectively. The 5 mg C/l set of experiments was repeated with the addition of 200 mg Na/l. The presence of the additional sodium caused the particles to grow unstable and form chemical floc during the particle formation experiments at all pH values, including high pH values where the suspensions had been stable when excess sodium was not added. Particle destabilization occurred without measurable differences in EPM.

Transmission electron microscopy and XRD analysis

The effect of 5, 50 and 500 mg C/l DIC on the structural properties of iron colloids formed at pH 8 is shown in TEM micrographs (Figure 11). Increasing the DIC produced colloids that appeared to consist of aggregates of small subunits which resulted in less dense overall features. In general, colloids formed in the 5 mg C/l DIC suspension appeared more as singular, dense masses with

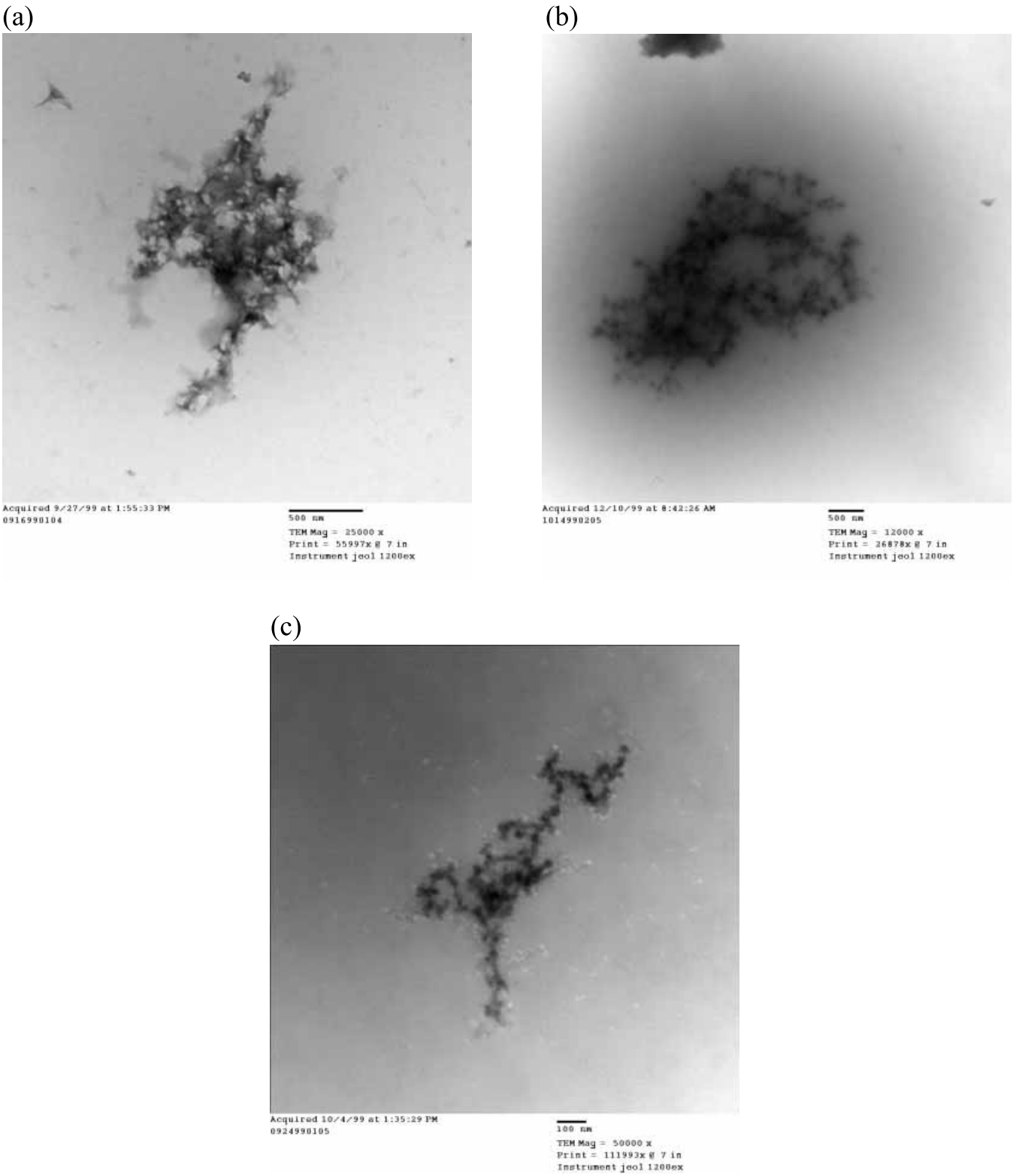

Figure 11 | Transmission electron micrograph of iron particles (1 mg Fe/l, pH 7.85 to 8.05, PO_2=0.122 atm, 22.5°C to 23.3°C), in (a) 5 mg C/l, (b) 50 mg C/l, and (c) 500 mg C/l DIC solutions.

slight crystalline properties as suggested by the appearance of some defined crystalline edges. XRD analysis of colloids showed that the particles were poorly ordered.

Particle size (based on filterable colour measurements) and suspension stability differences were attributed to iron particle EPM differences in most cases.

CONCLUSIONS

The following conclusions can be drawn from this study:

- Dissolved inorganic carbon concentration and pH affected the properties of iron particles and suspensions. Increasing the DIC concentration increased the turbidity and apparent colour of a fixed concentration of iron suspension below pH ~8.7. The turbidity and apparent colour of 5 mg Fe/l suspensions increased with increasing pH below ~8.7. Above pH 8.7 the influence of pH was dependent on whether an intermediate green solid formed.
- A measurable amount of DIC was incorporated in the structure of iron particles at pH values below 8 to 8.5.
- Inorganic carbon influenced the formation of redox sensitive, carbonate-containing green rust mineral at pH values greater than 8. This solid was present only for a short time. However, measurable amounts of inorganic carbon were not detected in the completely oxidized particles.
- Inorganic carbon altered the physical appearance and density of iron particles based on TEM micrographs. Even when inorganic carbon was not measured in the particle, the properties of the intermediate carbonate-containing green rust compound appeared to carry over to the final product. Structural and morphological differences are difficult to quantify, and the impact of such differences on corresponding suspension properties are not well known.
- An increase in inorganic carbon, and an increase in pH, decreased iron particle size based on filtration tests, particle size measurements and particle counts. The effect of inorganic carbon was limited to pH values below 8 to 8.5 where inorganic carbon was bound to the iron particles.

ACKNOWLEDGEMENTS

The authors wish to thank Barbara Francis, James Doerger and Keith Kelty for water quality analysis, Ian Laseke, Christy Frietch, Son Cao and Christina Feld from the U.S. Environmental Protection Agency (USEPA) for their assistance in operating the experimental apparatus. We would also like to thank Michael Schock and Matthew Magnuson, also with the USEPA, and Pankaj Sarin of the University of Illinois for their thoughts and discussions.

Mention of trade names or commercial products is for explanatory purposes only, and does not constitute endorsement or recommendation for use by the United States Environmental Protection Agency.

REFERENCES

APHA, AWWA & WEF 1995 *Standard Methods for the Examination of Water and Wastewater*, 19th Edn. American Public Health Association, Washington, DC.

ASTM 1996 Standard practices for identification of crystalline compounds in water-formed deposits by X-ray diffraction. In *1996 Annual Book of ASTM Standards*, Vol. 11.02, pp. 18–26. American Society for Testing and Materials, Conshohocken, PA.

Bachhuber, K. & Frosch, D. 1983 Melamine resin, a new class of water-soluble embedding media for electron microscopy. *J. Microsc.* **130**, 1.

Bier, M. 1959 *Electrophoresis: Theory, Methods and Application*. Academic Press, New York.

Buffle, J., De Vitre, R. R., Perret, D. & Leppard, G. G. 1989 Physico-chemical characteristics of a colloidal iron phosphate species formed at the oxic-anoxic interface of a eutrophic lake. *Geochim. Cosmochim. Acta* **53**, 399.

Carlson, L. & Schwertmann, U. 1981 Natural ferrihydrites in surface deposits from Finland and their association with silica. *Geochim. Comochim. Acta* **45**, 421.

Chambers, R. M. & Odum, W. E. 1990 Porewater oxidation, dissolved phosphate, and the iron curtain. *Biogeochemistry* **10**(1), 37.

Crosby, S. E., Glasson, D. R., Cuttler, A. H., Butler, I., Turner, D. R., Whitfield, M. & Millward, G. E. 1983 Surface areas and porosities of Fe(III)-and Fe(II) derived oxyhydroxides. *Environ. Sci. Technol.* **17**, 709.

Davis, J. A. 1982 Adsorption of natural dissolved organic matter at the oxide/water interface. *Geochim. Cosmochim. Acta* **46**, 2381.

Drissi, S. H., Refait, P., Abdelmoula, M. & Génin, J. M. R. 1995 The preparation and thermodynamic properties of Fe(II)-Fe(III) hydroxide-carbonate (green rust I); Pourbaix diagram of iron in carbonate-containing aqueous media. *Corros. Sci.* **37**(12), 2025.

Edwards, M. 1994 Chemistry of arsenic removal during coagulation and Fe-Mn oxidation. *J. Am. Wat. Wks Assoc.* **86**(9), 64.

Frosch, D. & Westphal, C. 1989 Melamine resins and their application in electron microscopy. *Electron Micros. Rev.* **2**, 231.

Fuller, C. C., Davis, J. A. & Waychunas, G. A. 1993 Surface chemistry of ferrihydrite: Part 2. Kinetics of arsenate adsorption and coprecipitation. *Geochim. Cosmochim. Acta* **57**, 2271.

Gshwend, P. M. & Reynolds, M. D. 1986 Monodisperse ferrous phosphate colloids in an anoxic groundwater plume. *Contaminant Hydrology* **1**, 309.

Gu, B., Schmitt, J., Chen, Z. & Liang, L. 1994 Adsorption and desorption of natural organic matter on iron oxide: mechanisms and models. *Environ. Sci. Technol.* **28**(1), 38.

Hach Company 1990 *DR/2000 Spectrophotometer Instrument Manual.* Loveland, CO.

Hansen, H. C. B. 1989 Composition, stabilization, and light absorption of Fe(II)Fe(III) hydroxy carbonate (green rust). *Clay Miner.* **24**, 663.

He, Q. H., Leppard, G. G., Paige, C. R. & Snodgrass, W. J. 1996 Transmission electron microscopy of a phosphate effect on the colloid structure of iron hydroxide. *Water Res.* **30**(6), 1345.

Hunter, R. J. 1981 *Zeta Potential in Colloid Science*. Academic Press, London.

James, A. M. 1991 Chapter 9: Charge properties of microbial cell surfaces. In *Microbial Cell Surface Analysis—Structural and Physicochemical Methods*, pp. 223–250. VCH Publishers Inc., New York, NY.

Kovacevic, D., Pohlmeir, A., Obas, G., Narres, H. D. & Kallay, M. J. N. 2000 The adsorption of lead species on goethite. *Colloids & Surfaces A: Phys. & Eng. Aspects* **166**, 225.

Landa, E. R. & Gast, R. G. 1973 Evaluation of crystallinity in hydrated ferric oxides. *Clay Miner.* **21**, 121–130.

Laxen, D. P. H. 1985 Trace metal adsorption/coprecipitation on hydrous ferric oxide under realistic conditions. *Wat. Res.* **19**, 1229.

Legrand, L., Sanvoye, S., Chausse, A. & Messina, R. 2000 Study of oxidation products formed on iron in solutions containing bicarbonate/carbonate. *Electrochemica Acta* **46**, 111.

Machesky, M. L., Bischoff, B. L. & Anderson, M. A. 1989 Calorimetric investigation of anion adsorption onto goethite. *Environ. Sci. Technol.* **23**, 580.

Mayer, T. D. & Jarrell, W. M. 2000 Phosphorous sorption during iron(II) oxidation in the presence of dissolved silica. *Wat. Res.* **34**(16), 3949.

Nomizu, T. & Mizuike, A. 1986 Electron microscopy of submicron particles in natural waters: specimen preparation by centrifugation. *Mikrochim. Acta* **1**, 65.

Odum, W. E. 1988 Comparative ecology of tidal freshwater and salt marshes. *Ann. Rev. Ecol. Syst.* **19**, 147–176.

Parks, G. A. 1965 The isoelectric points of solid oxides, solid hydroxides, and aqueous hydroxo complex systems. *Chem. Rev.* **65**, 177.

Perret, D., Leppard, G. G., Muller, M., Belzile, N., De Vitre, R. & Buffle, J. 1991 Electron microscopy of aquatic colloids: non-perturbing preparation of specimens in the field. *Wat. Res.* **25**, 1333.

Pierce, M. L. & Moore, C. B. 1980 Adsorption of arsenite on amorphous iron hydroxide from dilute aqueous solution. *Environ. Sci. & Technol.* **14**(2), 214.

Pontius, F. W. 1992 A current look at the federal drinking water regulations. *J. Am. Wat. Wks Assoc.* **84**(3), 36.

Schwertmann, U. & Cornell, R. M. 1991 *Iron Oxides in the Laboratory: Preparation and Characterization*. VCH, New York, NY.

Schwertmann, U. & Fechter, H. 1994 The formation of green rust and its transformation to lepidocrocite. *Clay Min.* **29**, 87.

Schwertmann, U. & Fischer, W. R. 1973 Natural ''amorphous'' ferric hydroxide. *Geoderma* **10**, 237.

Schwertmann, U. & Thalmann, H. 1976 The influence of [Fe(II)], [Si], and pH on the formation of lepidocrocite and ferryhidrite during the oxidation of $FeCl_2$ solutions. *Clay Min.* **11**, 189.

Seamon, J. C., Bertsch, P. M. & Strom, R. N. 1997 Characterization of colloids mobilized from southeastern coastal plain sediments. *Environ. Science & Technol.* **31**(10), 2782.

Skoog, D. A. & West, D. M. 1963 *Fundamentals of Analytical Chemistry*, 2nd Edn. Holt, Rinehart & Winston, Inc., New York.

Tejedor-Tejedor, M. I., Yost, E. C. & Anderson, M. A. 1992 Characterization of benzoic and phenolic complexes at the goethite/aqueous solution interface using cylindrical internal reflection Fourier transform infrared spectroscopy. 2. Bonding structures. *Langmuir* **8**(2), 525.

Tipping, E. & Cooke, D. 1981 The effects of absorbed humic substances on the surface charge of goethite in freshwaters. *Geochim. Cosmochim. Acta* **46**, 75.

van Gaans, P. F. M. 1989 WATEQX—A restructured, generalized, and extended FORTRAN 77 computer code and database format for the WATEQ aqueous chemical model for trace element speciation and mineral saturation, for use on personal computers or mainframes. *Comp. & Geosci.* **15**(6), 843.

Waychunas, G. A., Rea, B. A., Fuller, C. C. & Davis, J. A. 1993*a* Surface chemistry of ferrihydrite: Part 1. EXAFS studies of the geometry of coprecipitated and adsorbed arsenate. *Geochim. Cosmochim. Acta* **57**, 2251.

Waychunas, G. A., Davis, J. A. & Fuller, C. C. 1993*b* Surface chemistry of ferrihydrite: Part 2. Kinetics of arsenate adsorption and coprecipitation. *Geochim. Cosmochim. Acta* **57**, 2271.

Waychunas, G. A., Davis, J. A. & Fuller, C. C. 1995 Geometry of sorbed arsenate on ferrihydrite and crystalline FeOOH: Re-evaluation of EXAFS results and topological factors in predicting sorbate geometry, and evidence for monodentate complexes. *Geochim. Cosmochim. Acta* **59**(17), 3655.

Yost, E. C., Tejedor-Tejedor, M. I. & Anderson, M. A. 1990 In situ CIR-FTIR characterization of salicylate complexes at the goethite/aqueous solution interface. *Environ. Sci. Technol.* **24**, 822.

Zinder, B., Furrer, G. & Stumm, W. 1986 The coordination chemistry of weathering: II. Dissolution of Fe(II) oxides. *Geochim. Cosmochim. Acta* **50**, 1861.

First received 17 April 2002; accepted in revised form 29 July 2002